HHS Public Access

Author manuscript

J Invest Dermatol. Author manuscript; available in PMC 2016 May 18.

Published in final edited form as:

J Invest Dermatol. 2015 December ; 135(12): 3086–3095. doi:10.1038/jid.2015.280.

Defining the contribution of MC1R physiological ligands to ATR phosphorylation at Ser435, a predictor of DNA repair in melanocytes

Stuart G. Jarrett[1], **Erin M. Wolf Horrell**[1,2], **Mary C. Boulanger**[3], and **John A. D'Orazio**[1,2,4,5,6,*]

[1]Markey Cancer Center, University of Kentucky College of Medicine, Lexington, Kentucky 40536, USA

[2]Department of Physiology, University of Kentucky College of Medicine, Lexington, Kentucky 40536, USA

[3]Department of Dietetics and Human Nutrition, University of Kentucky College of Medicine, Lexington, Kentucky 40536, USA

[4]Department of Toxicology and Cancer Biology, University of Kentucky College of Medicine, Lexington, Kentucky 40536, USA

[5]Department of Pharmacology and Nutritional Sciences, University of Kentucky College of Medicine, Lexington, Kentucky 40536, USA

[6]Department of Pediatrics, University of Kentucky College of Medicine, Lexington, Kentucky 40536, USA

Abstract

The melanocortin 1 receptor (MC1R), a G_S-coupled receptor that signals through cAMP and PKA, regulates pigmentation, adaptive tanning, and melanoma resistance. MC1R-cAMP signaling promotes PKA-mediated phosphorylation of ataxia telangiectasia and rad3-related (ATR) at Ser435 (ATR-pS435), a modification that enhances nucleotide excision repair (NER) by facilitating recruitment of the XPA protein to sites of UV-induced DNA damage. High-throughput methods were developed to quantify ATR-pS435, measure XPA-photodamage interactions and assess NER function. We report that melanocyte stimulating hormone (α-MSH) or adrenocorticotropic hormone (ACTH) induce ATR-pS435, enhance XPA's association with UV-damaged DNA and optimize melanocytic NER. In contrast, MC1R antagonists agouti signaling protein (ASIP) or human β-defensin 3 (HBD3) interfere with ATR-pS435 generation, impair the XPA-DNA interaction and reduce DNA repair. Although ASIP and HBD3 each blocked α-MSH-mediated induction of the signaling pathway, only ASIP depleted basal ATR-pS435. Our findings confirm that ASIP diminishes agonist-independent MC1R basal signaling whereas HBD3 is a

*Author to whom correspondence should be addressed: John D'Orazio, M.D., Ph.D., Associate Professor of Pediatrics, University of Kentucky College of Medicine, Markey Cancer Center, Combs Research Building 204, 800 Rose Street, Lexington, KY 40536-0096, Phone (859) 323-6238, Fax: (859) 257-8940, ; Email: jdorazio@uky.edu

CONFLICT OF INTEREST

The authors state no conflict of interest.

neutral MC1R antagonist that blocks activation by melanocortins. Furthermore, our data suggest that ATR-pS435 may be a useful biomarker for the DNA repair-deficient MC1R phenotype.

Keywords

Ataxia telangiectasia and Rad3-related (ATR); cAMP-dependent protein kinase A; melanocortin 1 receptor (MC1R); Nucleotide excision repair (NER); ultraviolet-radiation; melanocyte stimulating hormone (α-MSH); agouti stimulating protein (ASIP) and β-defensin 3 (HBD3)

INTRODUCTION

The melanocortin 1 receptor (MC1R) is critical to melanocyte physiology, influencing resistance to malignant degeneration (Valverde *et al.,* 1996), pigmentation (Valverde *et al.,* 1995), the adaptive tanning response (D'Orazio *et al.,* 2006) and UV resistance (Hauser *et al.,* 2006). MC1R is a G_s-coupled receptor that signals through cAMP and PKA-mediated mechanisms when activated by ACTH or α-melanocyte stimulating hormone (α-MSH). Engagement of MC1R with agonistic ligands induces a number of prodifferentiation pathways, including up-regulation of melanin synthesis and production of brown/black eumelanin instead of red/yellow pheomelanin (Abdel-Malek *et al.,* 2000; Abdel-Malek *et al.,* 2014). MC1R signaling is impacted by a variety of ligands which together regulate MC1R-cAMP responses. The agouti signaling protein (ASIP) functions as an inverse agonist for MC1R decreasing MC1R basal signaling (Suzuki *et al.,* 1997), while human β-defensin 3 (HBD3) functions as a neutral antagonist blunting the effects of other MC1R ligands (Candille *et al.,* 2007; Nix *et al.,* 2013). In humans, MC1R is highly polymorphic with more than 70 variants, a few of which blunt MC1R-cAMP signaling responses (Garcia-Borron *et al.,* 2014). At least five “red hair color” (RHC) single nucleotide polymorphisms (MC1R-D84E, -R142H, -R151C, -R160W, and -D294H) are associated with red hair, freckling, fair skin and UV sensitivity (Valverde *et al.,* 1995).

Though MC1R loss is clearly linked with defective basal and adaptive pigmentation (D'Orazio *et al.,* 2006), MC1R signaling also protects melanocytes against carcinogenesis independent of pigmentation. Most notably, cAMP facilitates the repair of UV-induced damage via enhancing nucleotide excision repair (NER) (Hauser *et al.,* 2006; Kadekaro *et al.,* 2010). The importance of NER for resistance to melanoma and other UV-induced cancers is evident by the natural history of XP patients who, because of homozygous loss of any of eight essential NER proteins, have more than a three-log higher risk of melanoma and keratinocyte malignancies (DiGiovanna and Kraemer, 2012). XPA is part of the core incision complex of NER and interacts with DNA along with other NER and damage response proteins (Kang *et al.,* 2011). Similarly, ATR is critical to UV DNA damage signaling (Matsuoka *et al.,* 2007) and is linked with NER (Lindsey-Boltz *et al.,* 2009). Recently we described a molecular link between α-MSH-MC1R signaling and the NER pathway involving both ATR and XPA (Jarrett *et al.,* 2014). Specifically, MC1R-cAMP signaling increased NER through PKA-mediated phosphorylation of ATR at S435 (ATR-pS435), which promoted ATR’s interaction with XPA to accelerate recruitment of the ATR-XPA complex to sites of photodamage. In this report, we examine how agonistic and antagonistic

ligands of MC1R affect ATR-pS435 generation, XPA-DNA interactions and NER efficiency. To accomplish this, two high-throughput fluorescence assays were developed. Using biotinylated peptides mimicking the primary sequence of ATR surrounding S435, we measured endogenous ATR phosphorylation following agonism/antagonism of MC1R. In addition, using a biotinylated synthetic construct utilized in the oligonucleotide retrieval assay (ORA) (Shen *et al.,* 2014), we studied the effect of MC1R agonism/antagonism on XPA or ATR's interactions with photolesion-containing DNA as well as functional effects on NER efficiency. We found that physiological ligands of MC1R regulate levels of ATR-pS435, XPA-photodamage association and NER activity. Antagonizing MC1R with either ASIP or HBD3 abolished ATR-pS435 production, impaired XPA-DNA associations and reduced NER efficiency. ASIP but not HBD3 downregulated basal levels of ATR-pS435 and NER capacity. Taken together, our study suggests that ATR-pS435 may be a useful biomarker for the DNA repair deficient MC1R phenotype and introduces two sensitive assays that enable quantification of ATR-pS435 and protein interactions with UV-damaged DNA.

RESULTS

ATR phosphorylation at S435 is a biomarker for MC1R function

cAMP-mediated enhancement of NER is dependent on phosphorylation of ATR on the S435 residue by PKA (Jarrett *et al.,* 2014). To evaluate whether phosphorylation of ATR can be used as a marker of MC1R function, we compared the ability of primary human melanocytes (PHMs), melanoma cells and HEK cells transfected with wild-type MC1R or mutant RHC variants (R160W and D294H; Supplemental Figure 1) to respond to α-MSH. A high-throughput fluorescence-based screening method was developed using a biotinylated peptide containing ATR-S435 and a phospho-specific anti-ATR-pS435 antibody. All lines expressing wild-type MC1R demonstrated dose-dependent increases in S435 phosphorylation when incubated with α-MSH or forskolin, a direct activator of adenylate cyclase (Figure 1 a,b and c). Phosphorylation of ATR at S435 closely correlated with cAMP generation (Supplemental Figure 2). In contrast, MC1R mutant cells failed to generate ATR-pS435 (Figure 1 d,e and f) and had blunted cAMP generation (Supplemental Figure 2) after α-MSH exposure, but showed robust responses to forskolin. Enzyme kinetics for PKA-mediated ATR phosphorylation were calculated across increasing peptide concentrations (Figure 2) and incubation times (Figure 3). α-MSH induced effective ATR-pS435 generation in cells expressing wild-type MC1R (Figure 2a,b and c and Supplemental Table 1). In contrast α-MSH yielded no measureable ATR phosphorylation in cells bearing MC1R-RHC (Figure 2d,e and f and Supplemental Table 1). Pharmacologic cAMP induction by forskolin rescued ATR-pS435 generation in each line irrespective of MC1R status and even surpassed the efficiency of α-MSH-MC1R signaling in MC1R-WT cells. Forskolin-induced generation of ATR-pS435 in PHMs occurred concomitantly with cAMP generation, CREB phosphorylation and tyrosinase expression (Supplemental Figure 3). A linear relationship between ATR-pS435 generation and amount of nuclear extract was confirmed (Supplemental Figure 4). Pre-immune rabbit serum did not recognize the peptide regardless of phosphorylation status, anti-pS435 ATR did not recognize a non-phosphorylatable

(S435A) peptide, and total-ATR recognized the peptide regardless of phosphostatus of S435 (Supplemental Figure 5).

To characterize the kinetics of PKA-mediated S435 phosphorylation, we tested the ability of PKA to directly phosphorylate ATR-S435 in a cell-free system using recombinant catalytically-active PKA. We noted dose- and time-dependent phosphorylation of the ATR S435 peptide (Figure 3a) but not the ATR A435 mutant peptide incapable of being PKA phosphorylated (Figure 3b). Addition of the PKA inhibitors H-89 or PKI abolished phosphorylation of S435 (Figure 3a), confirming the need for functional PKA activity. Enzyme kinetic studies demonstrated dose-dependent α-MSH-mediated increases in K_m values for the ATR S435 peptide (Figure 3c and Supplemental Table 2), but not for the mutant A435 peptide (Figure 3d and Supplemental Table 2). Taken together, these data strongly suggest that ATR-pS435 is a PKA-mediated biochemical event and is a functional biomarker for MC1R functionality.

Agouti stimulating protein and β-defensin 3 inhibit MSH induced ATR phosphorylation at S435

Next, we determined the impact of physiological MC1R antagonists on PKA-mediated ATR phosphorylation by measuring ATR-pS435 levels following α-MSH stimulation in the presence of various concentrations of either ASIP or HBD3. α-MSH promoted robust accumulation of ATR-pS435 in MC1R-WT PHM (Figure 4a and c); addition of increasing doses of either ASIP or HBD3 inhibited α-MSH-dependent ATR-pS435 generation as manifested by rightward shifts of EC_{50} values (Figure 4a and c) concomitantly with diminution of PKA activity as determined by CREBtide phosphorylation (Supplemental Figure 6). Furthermore, a dose-dependent inhibition of ATR-pS435 was observed following either ASIP or HBD3 treatment (Supplemental Figure 7). Of note, by comparing EC_{50} values between antagonists (Figure 4a and c), we found that ASIP was 15–20 times more effective than HBD3 at antagonizing α-MSH-mediated ATR-pS435 generation. Importantly, neither ASIP nor HBD3 impacted forskolin-mediated induction of ATR-pS435 (Figure 4b and d), suggesting that ASIP and HBD3 antagonize α-MSH-MC1R interactions rather than by inhibiting downstream cAMP responses.

Next, we evaluated the impact of other melanocyte growth factors on PKA-mediated ATR phosphorylation (Figure 4e). While α-MSH and ACTH each induced ATR-pS435, neither endothelin-1 (ET-1), stem cell factor (kit ligand; SCF) nor hepatocyte growth factor (HGF) promoted PKA-mediated ATR phosphorylation. Each growth factor, however, influenced known downstream effectors (Figure 4f), confirming their bioactivity in melanocytes. Taken together, these data suggest that both ASIP and HBD3 interfere with α-MSH-mediated but not pharmacologically (forskolin)-induced ATR-pS435 generation and that melanocyte growth factors that signal in an MC1R-independent manner do not promote PKA-mediated ATR phosphorylation.

MC1R agonists and antagonists regulate XPA-DNA interactions

Since phosphorylation of ATR at S435 enhances NER by recruiting XPA to UV-induced DNA damage (Jarrett *et al.*, 2014), we wished to determine how physiologic MC1R ligands

impact XPA recruitment to photolesions. To do so, the oligonucleotide retrieval assay (Shen *et al.*, 2014) was adapted to measure XPA-photodamage interactions using a technique that we have termed "oligonucleotide retrieval assay-immunoprecipitation" (ORiP). This assay relies on isolation of nuclear lysates, introduction of a biotinylated construct harboring a UV-damaged oligonucleotide, retrieval of the oligonucleotide by streptavidin and identification of bound proteins by Western blot. In this way, levels of oligonucleotide-bound XPA and ATR-pS435 were measured in nuclear lysates of either PHMs (Figure 5) or HEK cells expressing either MC1R-WT or MC1R-R151C (Supplemental Figure 8) and pre-treated as indicated. In each case, we observed no association of either XPA or ATR-pS435 with the undamaged oligonucleotide but there was robust binding of XPA or ATR-pS435 with UV-irradiated oligonucleotide. Low levels of either XPA (Figure 5a and b) or ATR-pS435 (Figure 5c and d) associated with the photodamage-containing oligonucleotide in unstimulated cells. Pre-treatment with α-MSH or forskolin, however, increased accumulation of both XPA (Figure 5a and b and Supplemental Figure 8) and ATR-pS435 (Figure 5c and d) roughly 3–4 fold above vehicle ($p \leq 0.05$). Incubation of PHMs with either ASIP or HBD3 reduced photodamage-associated XPA or ATR-pS435 to vehicle-treated levels (Figure 5a–d) and each was significantly reduced compared to α-MSH alone ($p \leq 0.05$). Immunodepleting ATR-pS435 abolished any benefit of α-MSH-MC1R-cAMP signaling on XPA-DNA interactions (Figure e and f), demonstrating the critical role of this phosphorylation event for cAMP-enhanced XPA recruitement to photodamage. These data suggest ASIP and HBD3 negatively impact XPA-photodamage interaction by reducing the efficiency of MC1R-cAMP signaling.

MC1R agonists and antagonists regulate NER activity

As XPA and ATR-pS435 recruitment to UV-damaged DNA is dependent upon effective MC1R signaling, we reasoned that MC1R ligands would regulate melanocytic NER. As described, the oligonucleotide retrieval assay (ORA) measures repair by PCR-based amplification of an oligonucleotide construct containing a single chemically-induced thymine dimer whose amplification depends on repair of the photodamage (Shen *et al.*, 2014). Using this method, the presence of the CPD was verified by Southwestern blotting (Figure 6a), however we adapted the assay by UV-irradiating the oligonucleotide substrate to generate both cyclopyrimidine dimers (CPDs) and [6-4]-photoproducts ([6-4]-PP) (Figure 6b). α-MSH pre-treatment enhanced the repair of DNA lesions in either PHM (Figure 6c,d,e,f) or in MC1R-transfected HEK293 cells (Supplemental Figure 9) compared to vehicle in a dose dependent-manner (Supplemental Figure 10; $p \leq 0.05$). However, when either ASIP (Figure 6c and d) or HBD3 (Figure 6e and f) were incubated together with α-MSH, the repair of UV-induced lesions was significantly delayed in either cell type (ASIP; at 10, 50 and 100 nM; $p \leq 0.05$ and HBD3 at 100 nM; $p \leq 0.05$). Indeed, NER activity inversely correlated with increasing concentrations of either ASIP or HBD3 (Figure 6g and h).

We further delineated the long-term effect of ASIP and HBD3 on ATR-pS435 and NER independent of α-MSH signaling. ASIP treatment reduced both ATR-pS435 levels and NER activity below basal levels ($p \leq 0.05$) whereas HBD3 had no significant impact on basal ATR-pS435 levels or NER activity (Figure 6h), suggesting that ASIP but not HBD3

downregulates basal MC1R signaling. Altogether, these data indicate that melanocyte NER is regulated by agonists and antagonists of MC1R and identifies ATR-pS435 as a potential biomarker for the DNA repair deficient MC1R phenotype.

DISCUSSION

MC1R, a susceptibility gene for melanoma, encodes a G_s-protein coupled receptor expressed on the surface of melanocytes. MC1R protects cells from malignant degeneration by directing synthesis of UV-blocking melanin and by promoting genomic stability through enhanced NER (Hauser *et al.*, 2006; Wong *et al.*, 2012). Despite the fact that we and others have found MC1R signaling to enhance melanocytic NER by optimizing the function of numerous DNA repair factors (Jagirdar *et al.*, 2013; Jarrett *et al.*, 2014; Smith *et al.*, 2008; Swope *et al.*, 2014), how cAMP coordinates DNA repair responses is still incompletely understood. We previously found that MC1R signaling promoted NER through cAMP-directed PKA-mediated phosphorylation of ATR on the S435 residue which in turn up-regulated ATR's physical association with XPA and directed XPA to sites of UV damage to accelerate repair of photoproducts and protect against UV-induced mutagenesis (Jarrett *et al.*, 2014). Herein we examined the role of MC1R agonists and antagonists in regulating ATR-pS435 generation, XPA's interactions with photodamage and on NER using high throughput assays. Using these methodologies, we determined that in PHMs, the ATR-XPA NER axis is heavily influenced by agonists and antagonists of MC1R, implying that melanocyte genomic stability is directly regulated by MC1R signaling status and concentrations of MC1R ligands in the local milieu. Historically, kinase assays have relied on autoradiographic measurement of ^{32}P-containing phosphate into protein targets of interest. A fluorescence-based method was developed for detecting ATR-pS435 *in vitro* using a 14-mer peptide corresponding to residues 428–441 of ATR that contains the S435 residue in the context of its native PKA recognition site and that is specifically and efficiently recognized by a phospho-specific (ATR-pS435) when phosphorylated by PKA. This assay facilitates the study of MC1R signaling events that regulate ATR-pS435 and detects picomolar concentrations of ATR-pS435 generated by MSH or forskolin which is similar in sensitivity to radiolabelled phosphorylation assays (Gopalakrishna *et al.*, 1992). Using this approach, enzyme kinetic studies revealed higher V_{max} and lower K_m values for forskolin-mediated ATR-pS435 compared to α-MSH. Physiologically, these different kinetic properties suggest the increased "cAMP load" generated by forskolin may enhance the capability of PKA to recognize ATR-S435 and/or impact how strongly PKA binds with the S435 substrate in agreement with prior reports that modulations in PKA activity treatment alter the affinity of the enzyme for its substrate (Paulucci-Holthauzen et al., 2006).

ASIP and HBD3 efficiently blocked α-MSH-mediated effects on ATR-S435 phosphorylation but had no impact on forskolin-directed ATR-S435 phosphorylation. ASIP down-regulated basal levels of ATR-pS435, consistent with it being an MC1R inverse agonist capable of downregulating ligand-independent MC1R signaling (Sanchez-Mas *et al.*, 2004; Scott *et al.*, 2002; Suzuki *et al.*, 1997). HBD3, however, had no discernable impact on constitutive levels of ATR-pS435, suggesting it may function as a neutral MC1R antagonist instead (Candille *et al.*, 2007; Swope *et al.*, 2012). To elucidate the functional effect of MC1R ligands on DNA repair, we adapted the oligonucleotide retrieval assay which

quantifies repair by PCR-based amplification (Shen *et al.*, 2014). In this assay, the presence of photoproduct(s) interfere with Taq polymerase, therefore the amount of amplification across the oligonucleotide will be proportional to clearance of photolesions by NER. We adapted this method by directly UV-radiating the oligonucleotide instead which resulted in more photodamage (both CPDs and [6-4]-PP) than could be generated by chemical synthesis of a single CPD alone. NER responses were regulated by MC1R status and ligand interactions, mirroring ATR-pS435 accumulation and XPA-DNA binding. Thus, α-MSH promoted NER while ASIP and HBD3 blocked α-MSH-mediated enhancement of repair. ASIP blunted repair of UV-induced DNA damage to a greater extent than HBD3, which is explained by the fact that ASIP has a greater ability to inhibit ATR-pS435 generation than HBD3.

We also determined how MC1R ligands impact the biochemical association of XPA and ATR-pS435 with UV photodamage by ORiP, an assay we developed which takes advantage of the biotinylated oligonucleotide utilized in the ORA to identify proteins associated with UV-damaged oligonucleotide. This assay identified XPA as a key downstream target of the α-MSH-MC1R-cAMP axis in melanocytes which corroborates our previous studies (Jarrett *et al.*, 2014) and confirms the suitability of ORiP for the study of DNA-protein interactions. α-MSH pre-treatment enhanced accumulation of XPA on the UV-damaged DNA oligonucleotide whereas ASIP and HBD3 each antagonized the interaction. Previous studies in other systems have shown XPA to associate with DNA damage in response to UV irradiation (Lindsey-Boltz *et al.*, 2014), however data presented here link MC1R agonists and antagonists with efficiency of XPA recruitment to damaged DNA. Given the essential roles of XPA in DNA repair and genome maintenance (Cimprich and Cortez, 2008; Sirbu and Cortez, 2013), our findings suggest that ligand-MC1R control of XPA interactions represents an important mechanism underlying MC1R-regulation of NER in melanocytes. Indeed, MC1R signaling may be an important event that primes early recruitment and assembly of XPA and possibly other DNA repair proteins to sites of UV damage.

Together, these findings support the hypothesis that MC1R/cAMP signaling controls melanocytic NER through downstream PKA-mediated ATR phosphorylation on S435 and recruitment of XPA to photodamage. Our data raise the possibility that in addition to loss-of-function MC1R polymorphisms that interfere with cAMP generation in melanocytes, dysregulated expression of ASIP or HBD3 in the skin may also impair DNA repair responses in melanocytes to heighten UV mutagenesis and melanoma risk. Intriguingly, multiple factors in UV damage responses have been shown to be regulated by cAMP (Jarrett *et al.*, 2014; Kadekaro *et al.*, 2012; Smith *et al.*, 2008; Swope *et al.*, 2014; Swope *et al.*, 2012; Wong *et al.*, 2012) and may therefore be impacted by MC1R signaling or antagonism. In conclusion, our studies shed light on NER regulation by MC1R ligands and identify ATR-pS435 as a potential biomarker for the DNA repair deficient MC1R phenotype.

MATERIALS AND METHODS

Cell lines, plasmids, recombinant proteins and UV exposure

Transformed cell lines SK-MEL-2, A375, and HEK293 (ATCC) and primary melanocytes (Coriell) were cultured in RPMI media containing 10% FBS. HEK293 cells were transfected

with either MC1R-WT, MC1R-R160W or D294H as described (Jarrett *et al.*, 2014). Recombinant ACTH (Bioworld), ASIP (BD Biosciences) and HBD3 (BD Biosciences) were used as indicated. UV at a dose of 10 J/m^2 was delivered to cell cultures with lamps emitting in the UVB range.

Antibodies

The ATR antibodies ATR-pS435 and ATR-S435 were generated against the peptides CPKRRR(pS or S)SSLNPS (Amsbio). Commercially available antibodies used were anti-[6-4]-PP (Cosmo.bio), anti-CPD (Kamiya), anti-XPA (Kamiya), anti-FLAG (Sigma-Aldrich), anti-pp38(Cell Signaling), anti-pcKit (Cell Signaling), and anti-pCREB (Cell Signaling).

Chromatin isolation and immunoblotting

Chromatin isolation and immuoblotting was performed as described (Jarrett *et al.*, 2014).

ATR-pS435 detection

ATR-S435 kinase assays were performed using biotinylated ATR peptide substrates, CPKRRRLSSSLNPS or CPKRRRLASSLNPS (Genscript). Reactions containing peptide substrate (10μM-100μM) were performed in strepavidin-coated 96 well plates by the addition of either 10 nM recombinant catalytic subunit of PKA enzyme (Invitrogen) or chromatin lysate (500μg) in 40 mM Tris-HCl (pH 7.5), 10 mM $MgCl_2$, 1 mM DTT, 100 μg/ml BSA and10 μM ATP. Kinase reactions were carried out at 30°C with gentle agitation and terminated by the addition of 10 μl of 100 mM EDTA at indicated times. PKA phosphorylation was measured with either anti-ATR-pS435. Detection was accomplished using an HRP-conjugated anti-rabbit secondary antibody (Abcam) for 1 h followed by the addition of QuantaBLu (Pierce). Measurement of relative fluorescence units (RFU) was detected with excitation and emission set at 315 and 400nm. The kinetic parameters of the phosphorylation reaction were calculated by nonlinear regression analysis with GraphPad Prism.

Oligonucleotide retrieval (ORA) and oligonucleotide retrieval-immunoprecipitation (ORiP)

ORA was adapted to contain a UV-exposed DNA fragment containing [6-4]-PP and CPDs rather than a single CPD as reported previously (Shen *et al.*, 2014). Synthetic oligonucleotides (Molecular Beacons) were assembled to form a 5′-biotinylated duplex DNA fragment that acts as a substrate for NER. A 30-nt oligonucleotide, 5′-CTCGTCAGCATCTTCATCATACAGTCAGTG-3′, was exposed to 1 J/m2 of UVC and was annealed and ligated with two oligonucleotides as described (Shen *et al.*, 2014). For ORiP, after indicated treatments, chromatin fractions were incubated with the biotinylated oligonucleotide in strepavidin-coated 96 well plates (Thermo-Scientific) (0.01 nM per well) for indicated times at 30°C. Wells were washed with 40 mM Tris-HCl (pH 7.5) containing 0.01% BSA (wash buffer) followed by fixation in 4% paraformaldehyde. After three washes, 2 μg of either anti-XPA or anti-ATR-pS435 was added for 1h. Detection was accomplished using an HRP-conjugated anti-rabbit secondary antibody (Abcam) for 1 h followed by the addition of QuantaBLu (Pierce) to each well for 10 min at 37°C. Measurement of relative

fluorescence units (RFU) was detected with excitation and emission set at 315 and 400 nm. For ORA, either the construct as described above or a 30-nt oligonucleotide, 5′-CTCGTCAGCATC**TT**CATCATACAGTCAGTG-3′, containing a single CPD (where CPD is marked in bold) was used as a substrate for NER (generously provided by Dr. S. Iwai, Osaka University, Japan) (Nishiguchi *et al.*, 2008; Shen *et al.*, 2014). After indicated treatments, nuclear lysates (50 μg) were incubated with the UV-damaged oligonucleotide for indicated times at 30°C. The oligonucleotides were purified with DNAeasy extraction kit (Qiagen) and streptavidin beads (Invitrogen). Presence of UVR-induced DNA polymerase–blocking lesions was assessed using real-time quantitative PCR as described (Shen *et al.*, 2014). NER activity was expressed as percentage repair and calculated from WCt values assigning an oligonucleotide exposed to UVC at time zero as 100% DNA damage.

Statistical Analysis

All statistical assays, Student's t tests, and one-way ANOVA were performed with GraphPad Prism 5.0. Data were considered statistically significant if p values were less than 0.05.

Supplementary Material

Refer to Web version on PubMed Central for supplementary material.

ACKNOWLEDGEMENTS

We thank Dr. S. Iwai for the generous gift of the CPD-containing substrate. This work was supported by the following NIH grants: R01 CA131075 and T32CA165990. We thank the Drury Pediatric Research Endowed Chair Fund, Melanoma Research Alliance, Wendy Will Case Cancer Research Fund, Markey Cancer Foundation, Children's Miracle Network, and Jennifer and David Dickens Melanoma Research Foundation.

REFERENCES

Abdel-Malek Z, Scott MC, Suzuki I, et al. The melanocortin-1 receptor is a key regulator of human cutaneous pigmentation. Pigment Cell Res. 2000; 13(Suppl 8):156–162. [PubMed: 11041375]

Abdel-Malek ZA, Swope VB, Starner RJ, et al. Melanocortins and the melanocortin 1 receptor, moving translationally towards melanoma prevention. Arch Biochem Biophys. 2014; 563:4–12. [PubMed: 25017567]

Candille SI, Kaelin CB, Cattanach BM, et al. A β-defensin mutation causes black coat color in domestic dogs. Science. 2007; 318:1418–1423. [PubMed: 17947548]

Cimprich KA, Cortez D. ATR: an essential regulator of genome integrity. Nature reviews. 2008; 9:616–627.

D'Orazio JA, Nobuhisa T, Cui R, et al. Topical drug rescue strategy and skin protection based on the role of Mc1r in UV-induced tanning. Nature. 2006; 443:340–344. [PubMed: 16988713]

DiGiovanna JJ, Kraemer KH. Shining a light on xeroderma pigmentosum. J Invest Dermatol. 2012; 132:785–796. [PubMed: 22217736]

Garcia-Borron JC, Abdel-Malek Z, Jimenez-Cervantes C. MC1R, the cAMP pathway, and the response to solar UV: extending the horizon beyond pigmentation. Pigment cell & melanoma research. 2014; 27:699–720. [PubMed: 24807163]

Gopalakrishna R, Chen ZH, Gundimeda U, et al. Rapid filtration assays for protein kinase C activity and phorbol ester binding using multiwell plates with fitted filtration discs. Anal Biochem. 1992; 206:24–35. [PubMed: 1456438]

Hauser JE, Kadekaro AL, Kavanagh RJ, et al. Melanin content and MC1R function independently affect UVR-induced DNA damage in cultured human melanocytes. Pigment Cell Res. 2006; 19:303–314. [PubMed: 16827749]

Jagirdar K, Yin K, Harrison M, et al. The NR4A2 nuclear receptor is recruited to novel nuclear foci in response to UV irradiation and participates in nucleotide excision repair. PLoS ONE. 2013; 8:e78075. [PubMed: 24223135]

Jarrett SG, Horrell EM, Christian PA, et al. PKA-Mediated Phosphorylation of ATR Promotes Recruitment of XPA to UV-Induced DNA Damage. Mol Cell. 2014; 54:999–1011. [PubMed: 24950377]

Kadekaro AL, Chen J, Yang J, et al. Alpha-melanocyte-stimulating hormone suppresses oxidative stress through a p53-mediated signaling pathway in human melanocytes. Mol Cancer Res. 2012; 10:778–786. [PubMed: 22622028]

Kadekaro AL, Leachman S, Kavanagh RJ, et al. Melanocortin 1 receptor genotype: an important determinant of the damage response of melanocytes to ultraviolet radiation. Faseb J. 2010

Kang TH, Reardon JT, Sancar A. Regulation of nucleotide excision repair activity by transcriptional and post-transcriptional control of the XPA protein. Nucleic acids research. 2011; 39:3176–3187. [PubMed: 21193487]

Lindsey-Boltz LA, Kemp MG, Reardon JT, et al. Coupling of human DNA excision repair and the DNA damage checkpoint in a defined in vitro system. J Biol Chem. 2014; 289:5074–5082. [PubMed: 24403078]

Lindsey-Boltz LA, Sercin O, Choi JH, et al. Reconstitution of human claspin-mediated phosphorylation of Chk1 by the ATR (ataxia telangiectasia-mutated and rad3-related) checkpoint kinase. J Biol Chem. 2009; 284:33107–33114. [PubMed: 19828454]

Matsuoka S, Ballif BA, Smogorzewska A, et al. ATM and ATR substrate analysis reveals extensive protein networks responsive to DNA damage. Science. 2007; 316:1160–1166. [PubMed: 17525332]

Nishiguchi K, Yamamoto J, Iwai S. Stereoselective formation of a cyclobutane pyrimidine dimer by using N4-acetyl protection of the cytosine base. Nucleic Acids Symp Ser (Oxf). 2008:437–438.

Nix MA, Kaelin CB, Ta T, et al. Molecular and functional analysis of human betadefensin 3 action at melanocortin receptors. Chem Biol. 2013; 20:784–795. [PubMed: 23790489]

Sanchez-Mas J, Hahmann C, Gerritsen I, et al. Agonist-independent, high constitutive activity of the human melanocortin 1 receptor. Pigment Cell Res. 2004; 17:386–395. [PubMed: 15250941]

Scott MC, Suzuki I, Abdel-Malek ZA. Regulation of the human melanocortin 1 receptor expression in epidermal melanocytes by paracrine and endocrine factors and by ultraviolet radiation. Pigment Cell Res. 2002; 15:433–439. [PubMed: 12453185]

Shen JC, Fox EJ, Ahn EH, et al. A rapid assay for measuring nucleotide excision repair by oligonucleotide retrieval. Sci Rep. 2014; 4:4894. [PubMed: 24809800]

Sirbu BM, Cortez D. DNA damage response: three levels of DNA repair regulation. Cold Spring Harb Perspect Biol. 2013; 5

Smith AG, Luk N, Newton RA, et al. Melanocortin-1 receptor signaling markedly induces the expression of the NR4A nuclear receptor subgroup in melanocytic cells. J Biol Chem. 2008; 283:12564–12570. [PubMed: 18292087]

Suzuki I, Tada A, Ollmann MM, et al. Agouti signaling protein inhibits melanogenesis and the response of human melanocytes to alpha-melanotropin. J Invest Dermatol. 1997; 108:838–842. [PubMed: 9182807]

Swope V, Alexander C, Starner R, et al. Significance of the melanocortin 1 receptor in the DNA damage response of human melanocytes to ultraviolet radiation. Pigment cell & melanoma research. 2014; 27:601–610. [PubMed: 24730569]

Swope VB, Jameson JA, McFarland KL, et al. Defining MC1R Regulation in Human Melanocytes by Its Agonist alpha-Melanocortin and Antagonists Agouti Signaling Protein and beta-Defensin 3. J Invest Dermatol. 2012; 132:2255–2262. [PubMed: 22572817]

Valverde P, Healy E, Jackson I, et al. Variants of the melanocyte-stimulating hormone receptor gene are associated with red hair and fair skin in humans. Nat Genet. 1995; 11:328–330. [PubMed: 7581459]

Valverde P, Healy E, Sikkink S, et al. The Asp84Glu variant of the melanocortin 1 receptor (MC1R) is associated with melanoma. Hum Mol Genet. 1996; 5:1663–1666. [PubMed: 8894704]

Wong SS, Ainger SA, Leonard JH, et al. MC1R variant allele effects on UVR-induced phosphorylation of p38, p53, and DDB2 repair protein responses in melanocytic cells in culture. J Invest Dermatol. 2012; 132:1452–1461. [PubMed: 22336944]

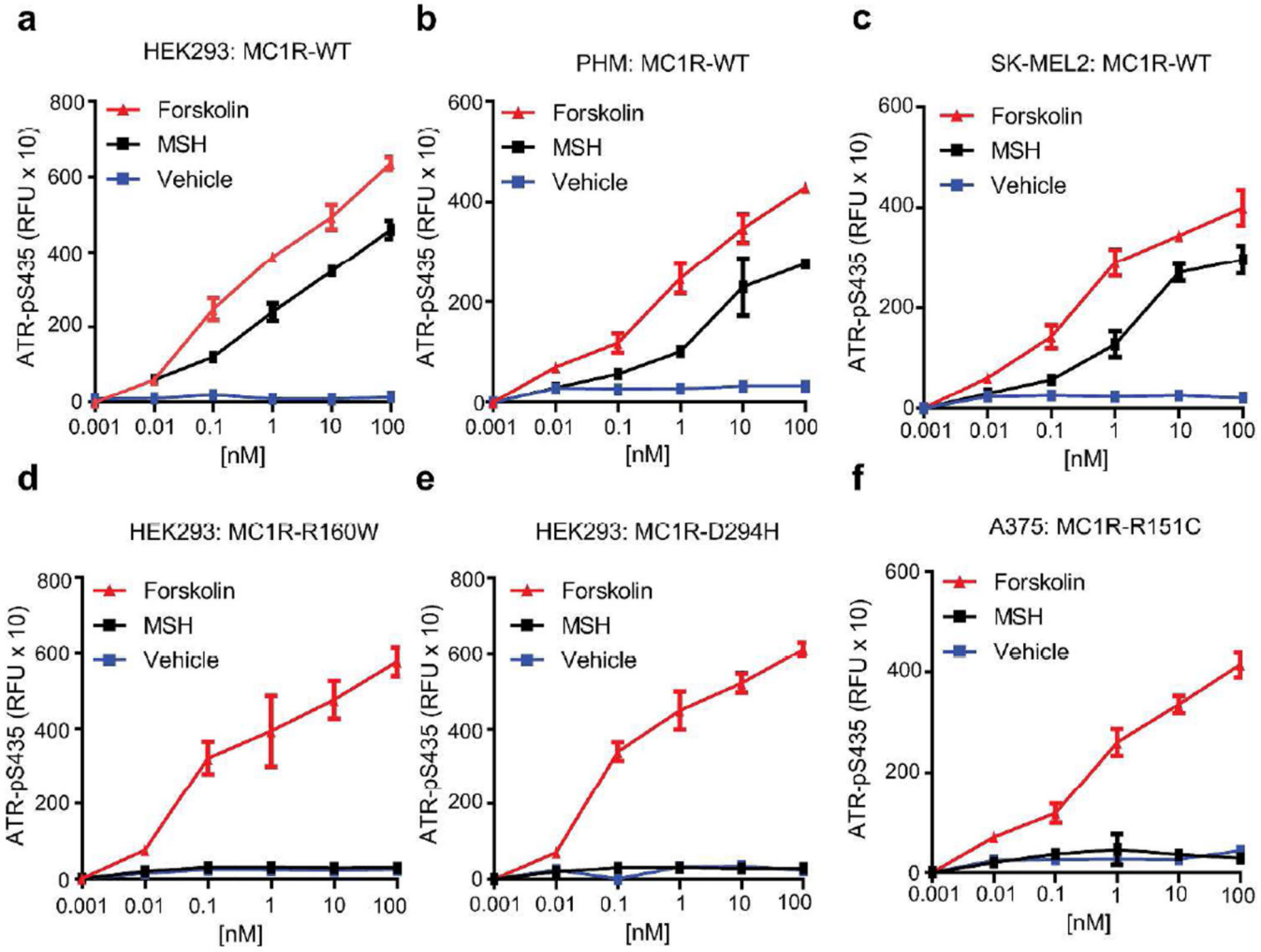

Figure 1. ATR phosphorylation at S435 is a biomarker of MC1R-cAMP signaling

Cell lysates were extracted from **(a)** HEK293-MC1R-WT, **(b)** PHM-MC1R-WT, **(c)** SK-MEL2-MC1R-WT, **(d)** HEK293-MC1R-R160W, **(e)** HEK293-MC1R-D294H and **(f)** A375-MC1R-R151C 30 minutes after treatment with indicated concentrations of either forskolin, α-MSH or vehicle. Wild-type and mutant MC1R expression in HEK293 cells were confirmed via Western blotting (Supplemental Figure 1). ATR-pS435 was measured using 10 μM CPKRRRLSSSLNPS as a substrate with anti-ATR-pS435 antibody coupled with fluorescence detection. Note that while forskolin promoted generation of ATR-pS435 across cell types, α-MSH did so only when MC1R was functional.

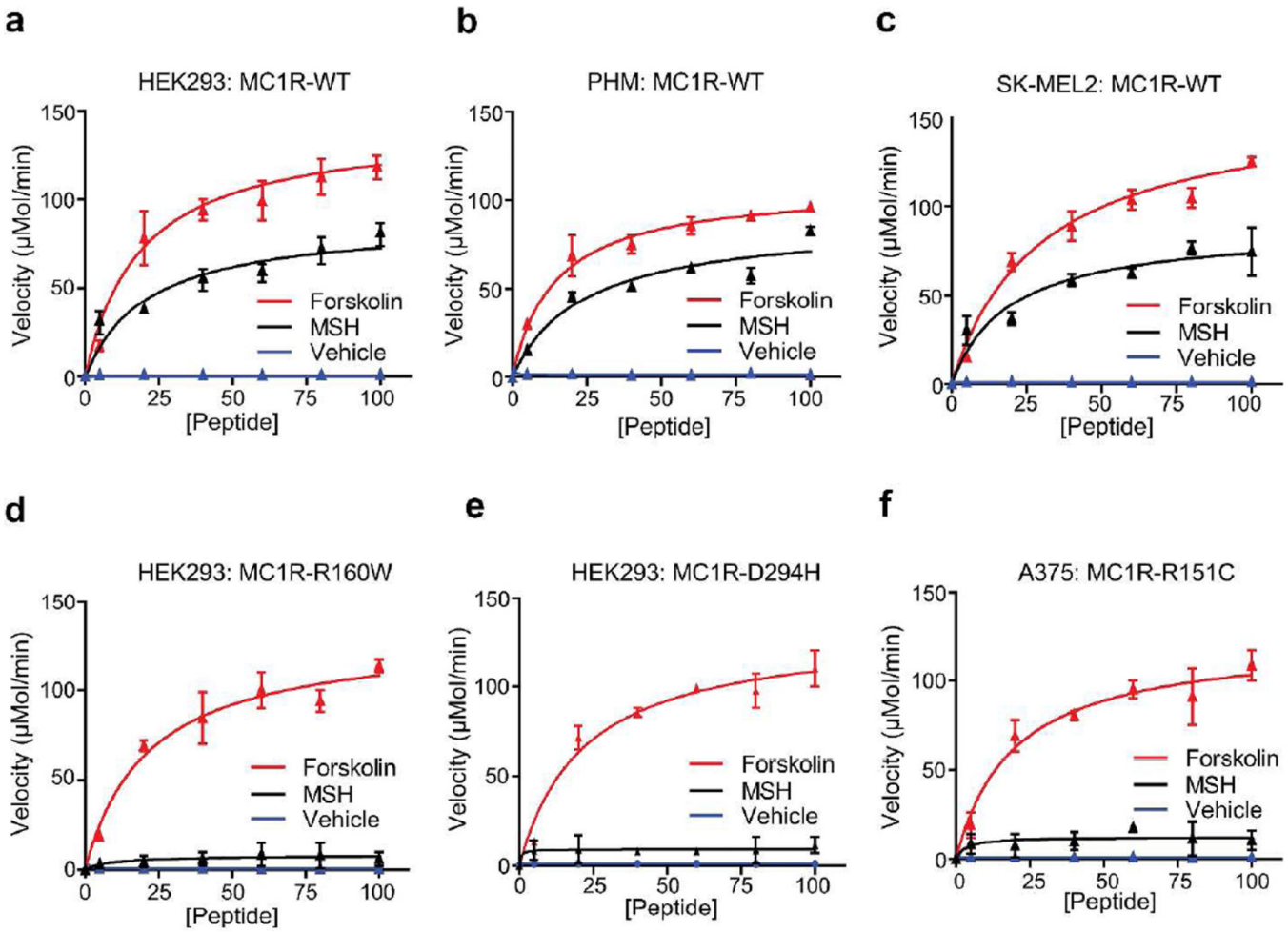

Figure 2. MC1R-cAMP signaling enhances the kinetics of ATR-pS435 generation

Cell lysates were extracted from **(a)** HEK293-MC1R-WT, **(b)** PHM-MC1R-WT, **(c)** SK-MEL2-MC1R-WT, **(d)** HEK293-MC1R-R160W, **(e)** HEK293-MC1R-D294H and **(f)** A375-MC1R-R151C following treatment with either forskolin (10 μM), α-MSH (100 nM) or vehicle for 30 minutes. ATR-pS435 was measured using the peptide CPKRRRLSSSLNPS (10 μM) as a substrate for 3 minutes (phosphorylation of the substrate was linear within this period). Kinetic parameters of the phosphorylation reaction were calculated by nonlinear regression analysis for the oligopeptide substrate using anti-ATR-pS435 antibody coupled with fluorescence detection. Mutant MC1R cells were unresponsive to α-MSH and were below the limits of detection. Linearity between ATR-pS435 and various amounts of whole cell extract were confirmed for all cell types (Supplemental Figure 4).

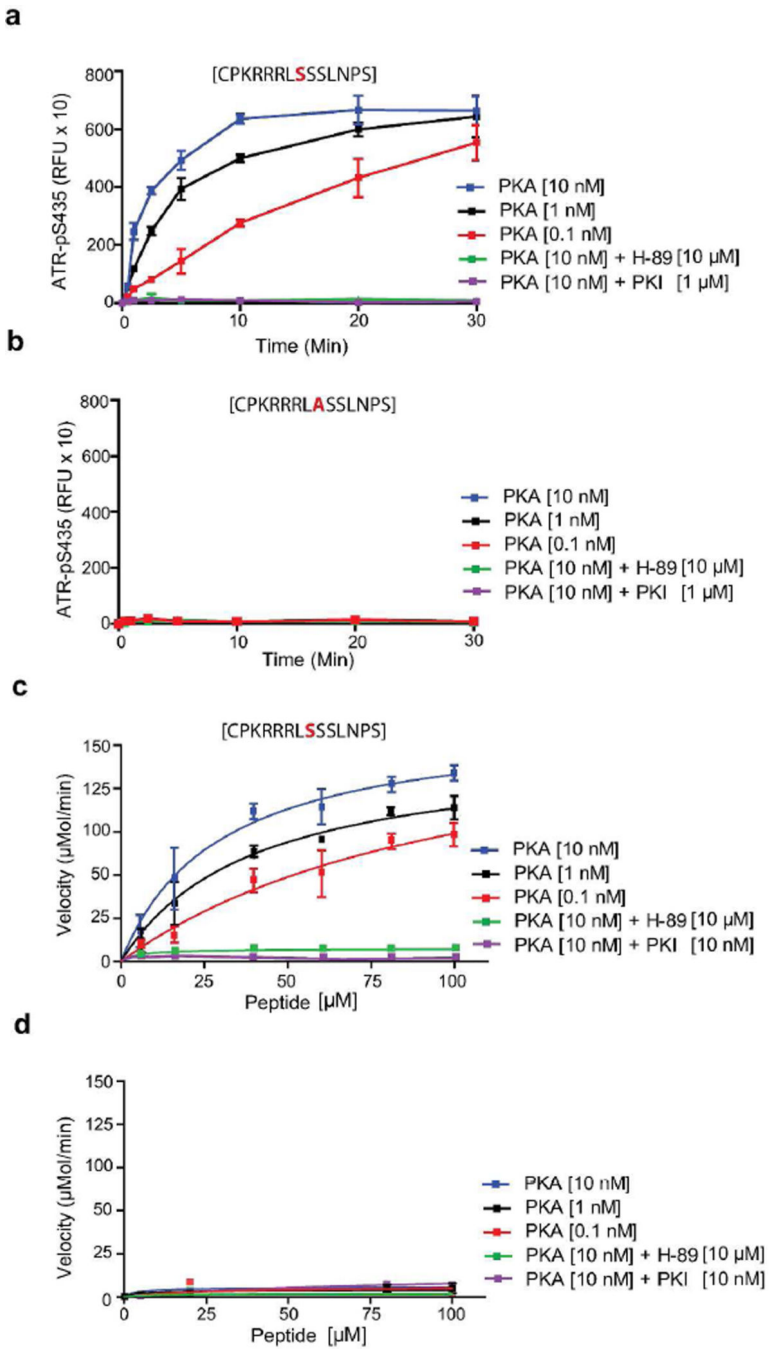

Figure 3. Dose and time response for PKA-mediated phosphorylation of ATR S435

Recombinant PKA (0, 0.1. 1 and 10 nM) or recombinant PKA (10 nM) with either H-89 (10 μM) or PKI (1 μM) were incubated with 10 μM peptide **(a)** CPKRRRLSSSLNPS or **(b)** CPKRRRLASSLNPS as substrates for up to 30 minutes. Extent of phosphorylation at Ser435 was measured by an anti-ATR-pS435 antibody. The kinetic parameters of the phosphorylation reaction were calculated by nonlinear regression analysis using 10 μM of **(c)** CPKRRRLSSSLNPS or **(d)** CPKRRRLASSLNPS as substrates and an anti-ATR-pS435

antibody coupled with fluorescence detection 3 minutes into each reaction (non-saturated conditions).

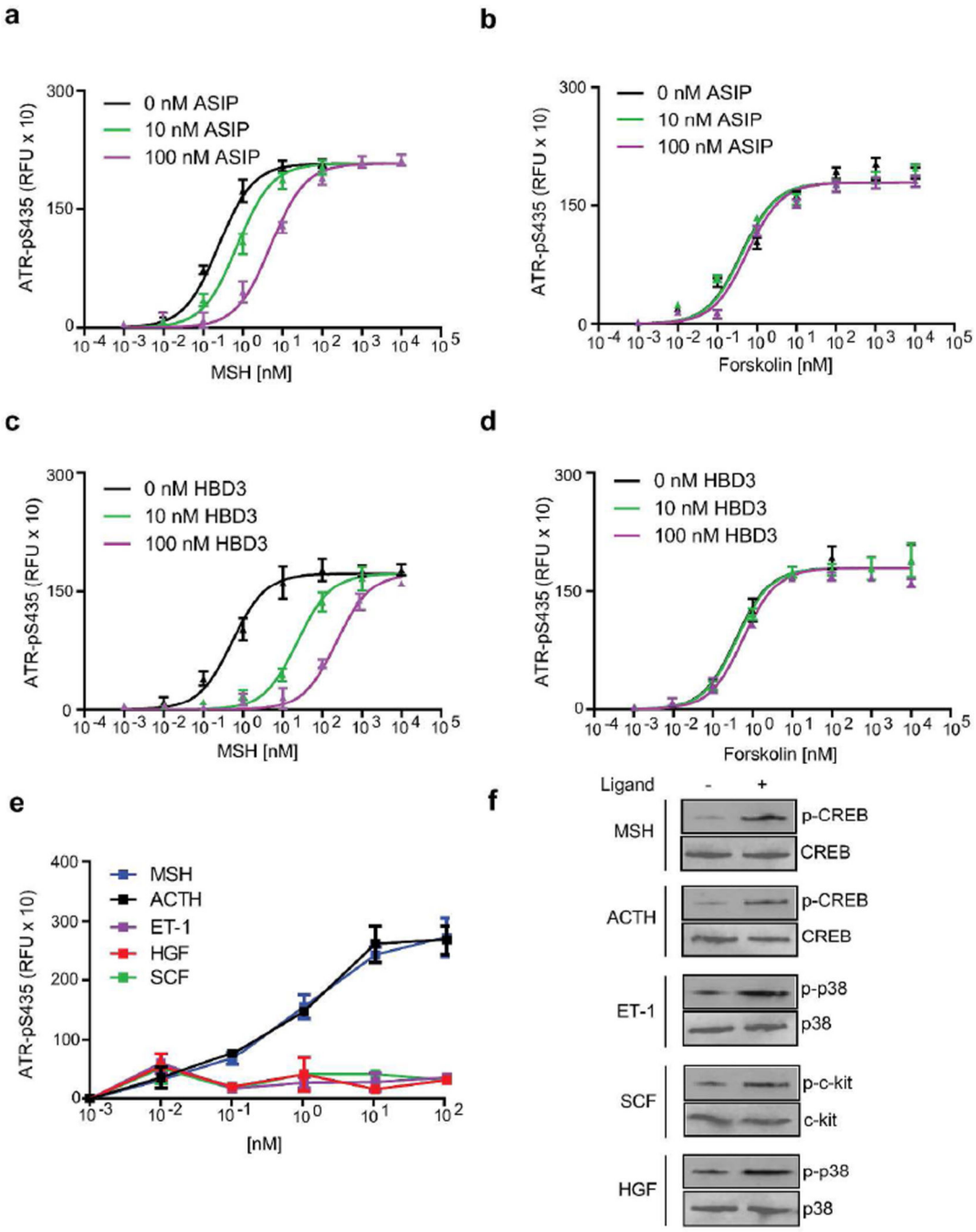

Figure 4. Antagonism of MC1R signaling by ASIP or HBD3 inhibit ATR-pS435 generation

Dose response analysis of ASIP mediated inhibition of **(a)** α-MSH (100 nM)- or **(b)** forskolin (10 μM) - generated ATR-pS435 or HBD3 inhibition of **(c)** α-MSH- or **(d)** forskolin-generated ATR-pS435. PHMs were treated with indicated concentrations of α-MSH or forskolin and either ASIP (0, 10 or 100 nM) or HBD3 (0, 10 or 100 nM) for 30 minutes before quantification of ATR-pS435 levels in whole cell lysates. **(e)** Dose response analysis of paracrine signaling factors on ATR-pS435 in PHMs (30 minute incubations) and **(f)** confirmation of specific ligand-mediated melanocyte responses in PHMs. ATRpS435 was

measured using the peptide, CPKRRRLSSSLNPS as a substrate and an anti-ATR-pS435 antibody coupled with fluorescence detection. EC_{50} values were calculated using sigmoidal dose-response curve fitting and defined as half maximal effective concentration of ATR-pS435 antagonism.

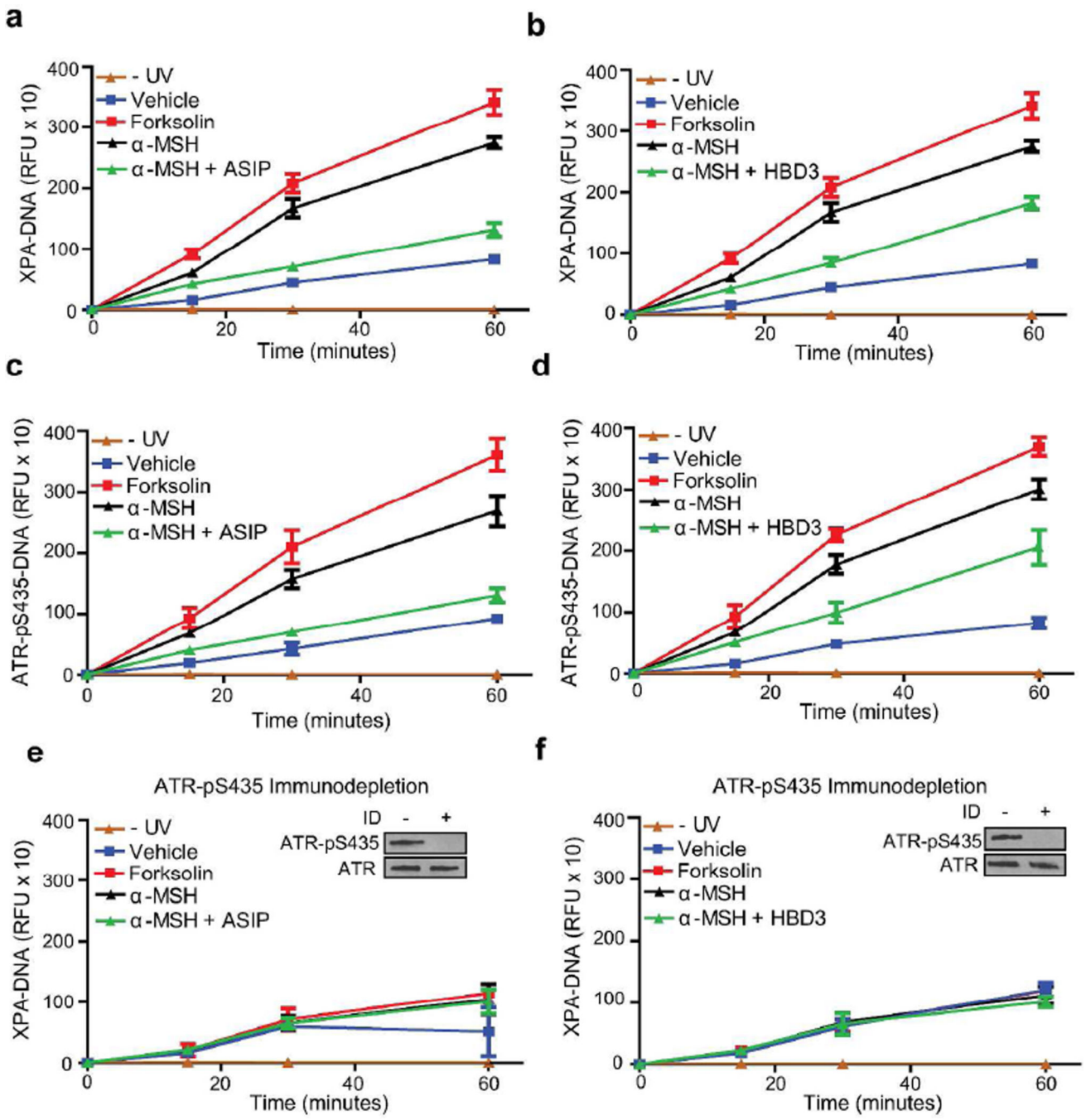

Figure 5. MC1R agonists and antagonists regulate XPA-DNA interactions following UV exposure

Wild-type MC1R PHMs were pre-treated with either forskolin (10 μM), α-MSH (100 nM), α-MSH (100 nM) + ASIP (100 nM) or HBD3 (100 nM) 30 minutes before UV exposure. PHMs that were not exposed to UV (−UV) were included to determine basal levels of damage. Nuclear extracts were incubated with a photoproduct containing 5′-biotinylated duplex DNA fragment that acts as a substrate for NER, as described in the Materials and Methods. The levels of **(a and b)** XPA, **(c and d)** ATR-pS435, **(e an f)** XPA (following immunodepletion (I.D) of ATR-pS435) bound to the DNA fragment was quantified as

described in Materials and Methods using fluorescence detection. Inset dispays ATR-pS435 and total ATR (10% input) protein levels.

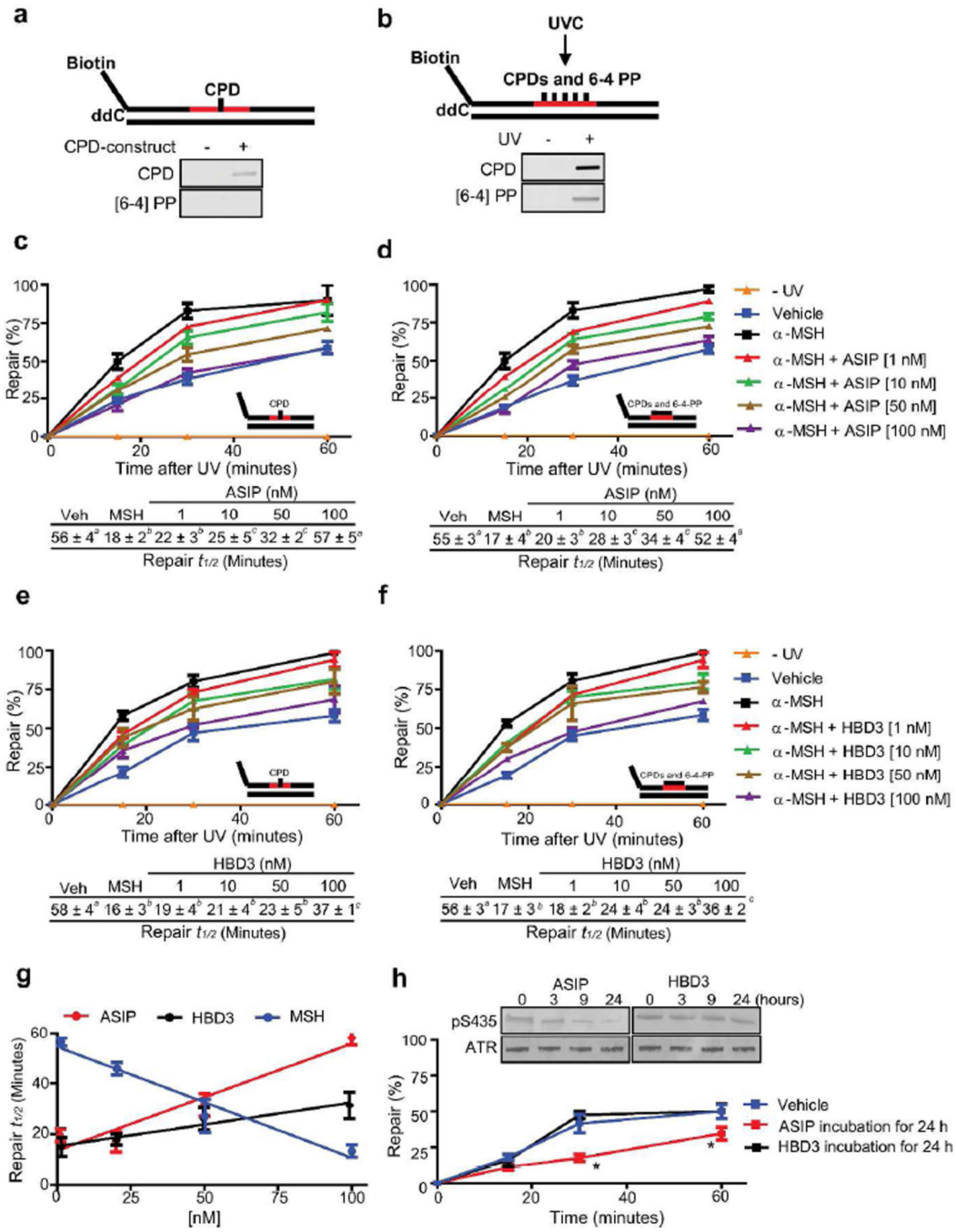

Figure 6. MC1R agonists and antagonists regulate NER

Wild-type MC1R PHMs were pre-treated with either α-MSH (100 nM), α-MSH (100 nM) + ASIP (1, 10, 50 or 100 nM) or α-MSH (100 nM) + HBD3 (1, 10, 50 or 100 nM) 30 minutes before UV exposure. The substrate for NER was either a **(a)** single CPD or **(b)** multi-photoproduct containing 5′-biotinylated duplex DNA fragment as described Materials and Methods. Nuclear extracts were incubated with substrate containing **(c and e)** single CPD or **(d and f)** multi-photoproducts. Values not sharing a common letter were significantly different as determined by one-way ANOVA. **(g)** Correlation of α-MSH, ASIP and HBD3

(1, 10, 50 and 100 nM) with DNA repair (expressed as $t_{1/2}$; the time taken to repair 50% of initial damage). **(h)** long-term incubation (24h) of ASIP (100 nM) and HBD3 (100 nM) on NER activity. Inset shows time course of ATR-pS435 following incubation with ASIP or HBD3. * signifies significant difference in repair $t_{1/2}$ between antagonist treated cells and vehicle treated cells ($p \leq 0.05$). Data are expressed as mean ± SEM.